Mesoscale Simulation of Rapid Soil Drying and Its Implications for Predicting Daytime Temperature

JOSEPH A. SANTANELLO JR.* AND TOBY N. CARLSON

Department of Meteorology, The Pennsylvania State University, University Park, Pennsylvania

(Manuscript received 15 October 1999, in final form 5 September 2000)

ABSTRACT

Rapid soil-surface drying, which is called ''decoupling,'' accompanied by an increase in near-surface air temperature and sensible heat flux, is typically confined to the top 1–2 cm of the soil, while the deeper layers remain relatively moist. Because decoupling depends also on a precise knowledge of fractional vegetation cover, soil properties, and soil water content, an accurate knowledge of these parameters is essential for making good predictions of temperature and humidity. Accordingly, some simulations centered on the Atmospheric Radiation Measurement Program Cloud and Radiation Test Bed Southern Great Plains site in Kansas and Oklahoma using a high-resolution substrate layer (Simulator for Hydrology and Energy Exchange at the Land Surface), the Fifth-Generation Pennsylvania State University–National Center for Atmospheric Research Mesoscale Model, and derived and default values for soil water content and fractional vegetation cover are presented. In so doing, the following points are made: 1) decoupling occurs only within certain threshold ranges of soil water content that are closely related to the soil type and 2) a knowledge of fractional vegetation cover derived from concurrent observations is necessary for capturing the spatial variation in rapid soil drying in forecast models.

1. Introduction

The interaction between the land surface and atmosphere is crucial for predicting daily maximum air temperature and humidity. Errors in predicting these variables result, in part, from incorrectly determining the partition of solar radiation into surface turbulent fluxes of heat and moisture. Studies have shown that the two most important land surface parameters that influence the surface energy budget are the near-surface soil water content (SWC) and the fraction of vegetation cover (Fr; Gillies et al. 1997; Sun and Bosilovich 1996). SWC is the most important soil characteristic governing fluxes at the air–soil interface, its impacts being much greater than those of soil albedo and soil type (Smith et al. 1994; McCumber and Pielke 1981). Moreover, surface heat fluxes are one order of magnitude more sensitive to the SWC profile than they are to the soil temperature profile (McCumber and Pielke 1981). SWC also plays a role in determining the heat and moisture fluxes within the soil (McCumber and Pielke 1981). The ability of new land surface schemes to handle more complex representations of the land surface highlights the need for more accurate estimates of SWC (and its vertical distribution).

Despite its importance in atmospheric forecast models, SWC still remains an elusive variable for real-time weather prediction because of the lack of field measurements, limited accuracy of remote sensing methods, and the overall heterogeneous nature of soil properties that cannot be captured by models with grid spacing on the order of kilometers (Capehart and Carlson 1997, hereinafter CC97; Capehart 1996). Soil moisture estimates made from space using microwave and thermal radiometry show some skill in assessing surface moisture on large spatial scales, but these techniques fail to capture the vertical variability in rapid soil drying that can occur as a result of a process discussed by CC97 called ''decoupling.''

Decoupling occurs when rapid soil drying takes place under intense sunshine, leading to a marked reduction in soil water content near the surface while leaving the deeper substrate relatively moist. Jackson (1973), CC97, and Carlson et al. (2000) show that this soil drying may be confined for a while to a very shallow substrate layer, perhaps less than 2 cm deep. Decoupling takes place during stage-2 (soil limited) evaporation (Idso et al. 1974; Brutsaert and Chen 1995) in which evaporation rates are limited by the efficiency of moisture diffusion from deeper to near-surface soil layers. Under these cir-

* Current affiliation: Department of Geography, Boston University, Boston, Massachusetts.

Corresponding author address: Joseph A. Santanello Jr., Dept. of Geography, Boston University, 442 Stone Science Bldg., Boston, MA 02215.
E-mail: sntnello@crsa.bu.edu

cumstances, surface estimates of SWC no longer represent a deep soil column, and current land surface process models may have insufficient vertical resolution to capture this kind of SWC profile, so that predicted afternoon temperatures may be grossly underestimated. Also, until recently, most atmospheric prediction models have simply employed climatological estimates to assign initial SWC.

Accurate initial vertical profiles of SWC are therefore necessary for making a correct prediction of surface fluxes. Hydrological models such as the Soil Hydrology Model (SHM) used in this study (Capehart and Carlson 1994; CC97; Crawford et al. 2000) can, in principle, provide a better estimate of SWC profiles (from the surface down to 2 m) than can climatic data, using conventional meteorological data. Moreover, they can capture small variations in soil drying that would otherwise produce serious errors in the surface fluxes if ignored.

Fractional vegetation cover describes the amount of solar radiation incident on bare soil surfaces within a specified area. For example, an Fr of 0.75 for a particular grid cell indicates that 75% of that grid cell is covered by vegetation and 25% by bare soil, which information land surface schemes then apply to the partitioning of surface processes such as net radiation (canopy vs soil), sensible heat flux, evaporation, and transpiration. Over dense vegetation, the latent heat flux is largely influenced by the plant (rather than the underlying soil surface) and responds more sensitively to the SWC in the root zone than at the soil surface. Decoupling events are thus expected to occur in low to moderately vegetated areas, although they may nevertheless take place at subgrid scales in bare patches between plants.

Fractional vegetation cover is a parameter utilized in most land surface schemes; however, it is almost always specified using climatological data. The advent and improvement of remotely sensed vegetation indices and the close relationship between Normalized Difference Vegetation Index (NDVI) data and Fr have enabled more accurate estimations of Fr to be produced at varying temporal and spatial scales (Choudhury et al. 1994; Gillies et al. 1997). These estimates of Fr must also be considered in prediction schemes in order to capture adequately the process of decoupling.

This paper addresses two questions: 1) under what circumstances will decoupling occur and 2) whether specifying more detailed and vertically resolved SWC and better estimates of Fr can capture the decoupling process in a coupled mesoscale model [The Fifth-Generation Pennyslvania State University (PSU)–National Center for Atmospheric Research (NCAR) Mesoscale Model (MM5)] with a land surface component [Simulator for Hydrology and Energy Exchange at Land Surface (SHEELS)]. Accordingly, we will first discuss the methodology of how initial SWC and Fr fields are generated. A more detailed description of input fields and soil physics of MM5/SHEELS is included in section 2. Sections 3 and 4 present the output from MM5/SHEELS, with particular attention to the impact of SWC and Fr on the simulations. A validation of air temperature simulations is described in section 5. Section 6 discusses these results and complicating issues and assesses the value of including these fields and finely resolved soil layers in land surface schemes.

2. Generation of input fields

a. Soil water content

SHM was specifically designed to provide initial soil water content fields to hydrological and meteorological forecast models using only conventional land use and meteorological data (Smith et al. 1994; Capehart 1996). Its advantages over using remotely sensed or climatological data for these mesoscale models make it desirable for producing regional-scale analyses of soil water content on a daily basis. More important, SHM can provide a highly resolved vertical profile of soil moisture for any combination of soil layers. Although it is a one-dimensional model, SHM is used here to generate SWC fields at 36-km grid spacing over most of the United States, from which MM5/SHEELS can be initialized. Previously, a 20-layer version of SHM with 10-cm vertical spacing was used to initialize soil moisture in MM5/Biosphere–Atmosphere Transfer Scheme (BATS; W. J. Capehart 1997, personal communication; Lapenta et al. 1998) and demonstrated improvement in predicting surface fluxes over those employing climatological (default) SWC values.

Still, this vertical spacing (10 cm) for soil moisture may produce large errors in surface fluxes, which depend on knowledge of the surface soil temperature in sparsely vegetated areas. Accordingly, a new higher-resolution 9-layer soil structure was specified in SHM in which the topmost layer is 2 cm deep (0–2 cm). Subsequent layers are staggered over different substrate depths: 3 (2–5), 5 (5–10), 15 (10–25), 25 (25–50), 25 (50–75), 25 (75–100), 50 (100–150), and 50 cm (150–200 cm depth), for a total of 2 m in depth. This new setup has three layers in the top 10 cm of soil, as opposed to a single 10-cm layer. The loss of resolution in the middle and lower soil layers is not thought to be a problem because of the more uniform nature of SWC in those deeper layers. Furthermore, tests on SHM have shown that subgrid-scale variability is smallest in deeper soil layers (Smith et al. 1994).

b. Fractional vegetation cover

NDVI is defined as

$$\text{NDVI} = (\alpha_{\text{IR}} - \alpha_{\text{VIS}})/(\alpha_{\text{IR}} + \alpha_{\text{VIS}}), \qquad (1)$$

where α_{IR} and α_{VIS} are the infrared and visible reflectances, respectively. A square root relationship between NDVI and Fr was first derived by Choudhury et al. (1994) and Gillies and Carlson (1995), and subsequently

used by Gillies et al. (1997) and Kustas and Norman (1999). From this result, it is now possible to derive reasonable estimates of Fr directly from NDVI. Carlson and Ripley (1997) show that calculating Fr from NDVI reduces the need for making an atmospheric correction to the remote sensing data. For this work, Fr fields were determined from the Earth Resources Observing Satellite (EROS) Data Center's 15-day Advanced Very High Resolution Radiometer composites of NDVI for the period 1990–98 using the method described by Gillies and Carlson (1995).[1]

An example of a final product of NDVI-derived fractional vegetation cover at 36-km grid spacing over the central United States in July can be seen in Fig. 1a. In contrast, the climatological analysis for this period, as generated by MM5 and based solely on subsurface temperature and date, illustrates the lower horizontal variability of default estimates of Fr (Fig. 1b).

c. SHEELS soil physics

The PSU–NCAR MM5 (Anthes and Warner 1978) was chosen as the forecast model for this study because of its wide use throughout the community and its ease of coupling with land surface schemes such as BATS (Dickinson et al. 1986). Recent modifications to the BATS land surface scheme have resulted in SHEELS (Lapenta et al. 1998). Of crucial importance in this model is the inclusion of highly resolved soil layers. Rather than the 0–10-cm top layer of BATS, SHEELS enables the soil properties, including soil moisture, to be specified in 1-cm layers. Accordingly, we specify five soil layers of equal depth in the upper 10 cm: 0–2, 2–4, 4–6, 6–8, and 8–10 cm. This arrangement can capture the details of rapid soil drying and the decoupling process. As in BATS, the root-zone depths are variable and based upon the land cover type.

The soil physics in SHEELS is nearly identical to that in BATS (and SHM), with the exception of the evaporation scheme. The temporal change in soil water content in each of the soil sublayers is determined by partitioning infiltration, evaporation, transpiration, diffusion, and gravitational drainage (and surface runoff and ponded water as residuals). The change in depth of water in soil layer d_i with time t can be expressed as

$$\partial d_i/\partial t = I_i - E_i - T_i, \quad (2)$$

where I_i, E_i, and T_i are the amounts of infiltration, evaporation, and transpiration attributed to layer i according to weighting functions. The proportion of infiltration for each layer is based on an inverted triangular weight extending from the surface to a depth determined by land cover type. The weighting functions for evaporation and transpiration are similar but are modified in proportion to the SWC within each layer. This approach allows for more evapotranspiration to be extracted from wet layers than from drier layers, relative to the weighting functions, which decrease from the surface downward. For evaporation, the depth of the triangle extends down to the same land cover–dependent depth as for infiltration, while the transpiration depth extends down through the root zone. Once the water depths have been calculated at each time step, the volumetric water contents θ_i are updated.

At each model time step and at each grid cell, the vertical fluxes of water between each layer are calculated using Darcy's law:

$$q_\theta = -k\partial h/\partial z, \quad (3)$$

where q_θ = vertical water flux, $k = k_s(\Theta)^{3+2b}$ = hydraulic conductivity, and $h = h(\Theta)$ = total hydraulic potential = $\psi + z = \psi_s(\Theta)^{-b} + z$ [where $\psi = \psi(\Theta)$ = hydraulic matric potential and z = gravitational potential, b = beta parameter (reciprocal of the pore size parameter λ), and Θ = relative soil water content = $(\Theta_i - \Theta_r)/(\Theta_s - \Theta_r)$]. The subscripts s and r refer to saturated and residual (wilting point) values, which are a function of soil type.

These formulations are based on the empirical parameterizations of soil properties by Clapp and Hornberger (1978), in which the exponential value b is recommended for each designated soil type. Therefore,

$$\begin{aligned} q_\theta &= -k\partial\psi/\partial z - k \\ &= -k_s(\Theta)^{3+2b}\partial[\psi_s(\Theta)^{-b}]/\partial z - k_s(\Theta)^{3+2b}. \end{aligned} \quad (4)$$

Applying mass continuity yields Richards's equation:

$$\partial\theta/\partial t \equiv -\partial q_\theta/\partial z = (\partial/\partial z)(k\partial\psi/\partial z) + \partial k/\partial z, \quad (5)$$

and expressing terms as functions of θ, we obtain

$$\partial\theta/\partial t = (\partial/\partial z)[D(\Theta)\partial\theta/\partial z] + (\partial k/\partial\Theta)\partial\theta/\partial z, \quad (6)$$

where $D(\theta) \equiv k\partial\psi/\partial\theta$ = the diffusion coefficient. The nonlinear dependence of SWC fluxes on the hydraulic conductivity and matric potential (or SWC itself), and therefore the beta parameter, is the cause of rapid soil drying and will be discussed further.

Isothermal vapor flux and thermally driven liquid and vapor fluxes occur near the soil surface. It should be noted that neither the SHM nor SHEELS accounts for these processes, and would require the addition of a heat diffusion equation to the liquid and vapor conservation equations, thus greatly increasing computational demand and complexity to a coupled model such as MM5/SHEELS. Studies have shown that in the absence of very moist or desiccated soil conditions, neglect of these thermally driven flows has only a 1% impact on surface evaporation, and isothermal liquid flux is the limiting process on evaporation (Milly 1982, 1984; Saravanapavan and Salvucci 2000). Furthermore, BATS and SHEELS resolve only a surface layer of 20 cm and deep

[1] A database of all the vegetation cover fields has been produced and at the time of writing was available online at http://www.essc.psu.edu/frac_veg.

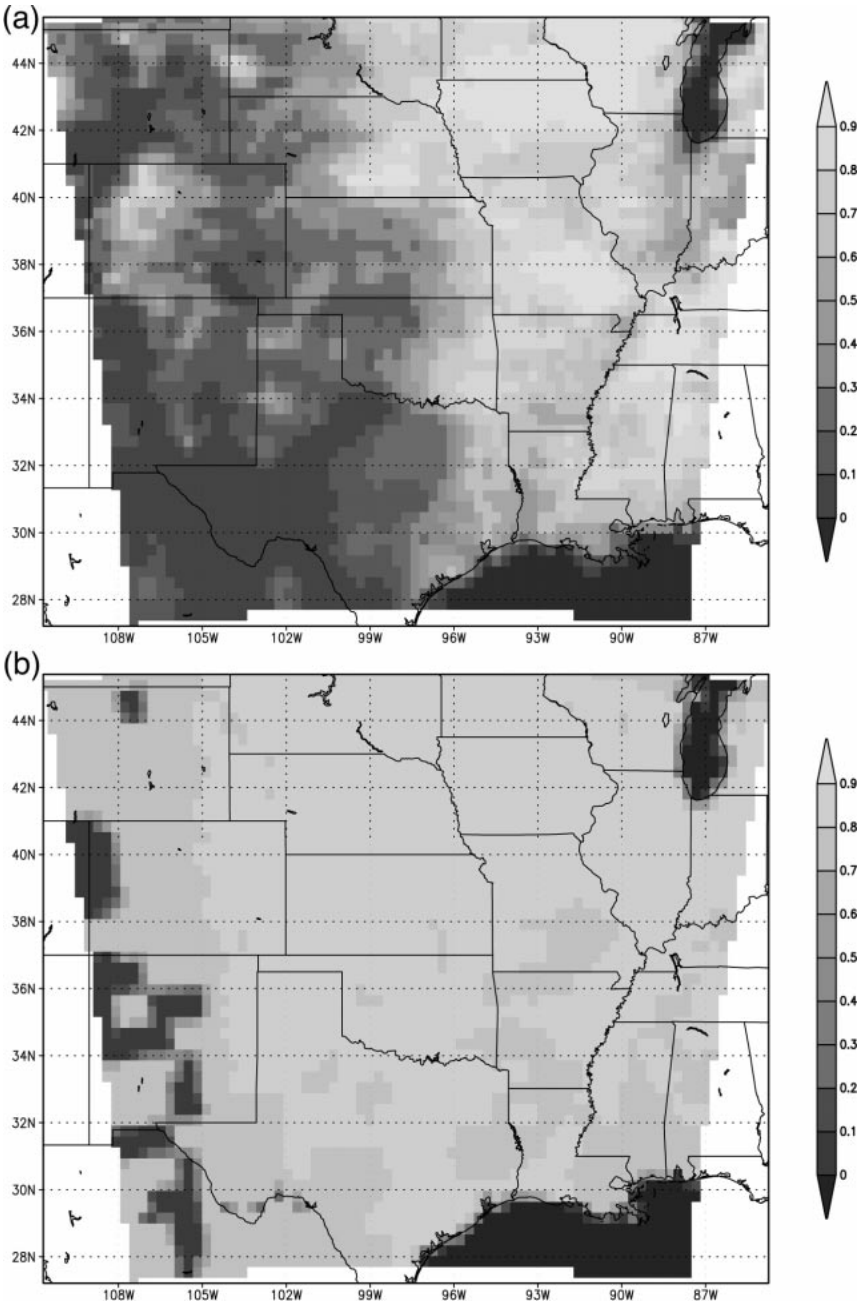

FIG. 1. Fractional vegetation cover over the central United States at 36-km grid spacing for 5–19 Jul 1996, derived from (a) 2-week composite NDVI measurements and (b) climatological estimates generated by default in MM5. Values range from 0.0 (0%) to 1.0 (100%) coverage, with brighter shades indicating higher values.

soil layer temperature using a force–restore approximation, which is not nearly enough to estimate realistic thermal gradients and fluxes. Results will show that the soil maintains a middle range of SWC throughout our simulations and does not reach saturated or desiccated conditions. For these reasons, the omission of thermally driven water flow in these simulations is not of primary concern and is not expected to produce first-order errors. A more complex and robust version of SHEELS will include a diffusion-based soil scheme in which temperatures will be evaluated at each sublayer, and the significance of these fluxes can be examined under a wide range of conditions.

The hysteretic nature of wetting and drying fronts observed in soils is not easily modeled, even by explicit soil hydrology models. Although hysteresis does have

TABLE 1. MM5/SHEELS simulations and the associated input fields initialized in each of the four simulations reported in the paper.

Simulation	SHEELS physics	GLCC land cover	STATSGO soil texture	Fractional vegetation cover	SHM soil moisture
1	No	No	No	No	No
2	Yes	Yes	Yes	No	No
3	Yes	Yes	Yes	Yes	No
4	Yes	Yes	Yes	Yes	Yes

an impact on soil water retention (ψ–Θ relationship) during sequential drying and wetting events, the 36-h simulation of a portion of one drying event (or a single scanning curve) performed here should not be a concern.

d. MM5/SHEELS simulations

MM5/SHEELS was run on three nested domains, a coarse outer grid of 36-km spacing (Figs. 1a,b), an interior grid of 12 km, and a finer mesh of 4-km grid spacing. The 4-km grid corresponds to the Atmospheric Radiation Measurement Program Cloud and Radiation Test Bed (ARM CART) Southern Great Plains (SGP) site covering central Kansas and Oklahoma, a region characterized by a large vegetation gradient from east to west. As such, the domain is optimal for this study, because the large and heterogeneous spatial variations in Fr and SWC provide a suitably large range of conditions for capturing the decoupling effect.

Dates were chosen from a period of abundant sunshine and light winds immediately following a moderate precipitation event. Initializing the model in these conditions provides sufficient time for MM5/SHEELS to simulate decoupling from a moist, but not saturated, soil profile. Accordingly, 1200 UTC 16 July 1996 was chosen as the start time of 36-h simulations spanning 2 days of strong solar heating and soil drying. National Centers for Environmental Prediction reanalysis data were used as the atmospheric boundary conditions and are not a major concern in our analyses.

Four MM5/SHEELS simulations for this 36-h period were made: 1) MM5 coupled with BATS using all climatological (default) parameters, 2) MM5 coupled with SHEELS using default vegetation cover and soil moisture profiles, 3) MM5 coupled with SHEELS using the derived Fr and default soil moisture profiles, and 4) MM5 coupled with SHEELS using the derived Fr and derived soil moisture profiles from SHM. These simulations and input fields are summarized in Table 1.

MM5/SHEELS divides its flux computation into a fraction of each grid cell covered by vegetation and a fraction covered by bare soil, then averages the two to produce a representative value for each grid cell (Smith et al. 1994). Fractional vegetation cover was initialized for these simulations using the appropriate 2-week NDVI composite and processed as described in section 2b. The derived Fr data were aggregated to the 36-km MM5 grid using a spatial average of 1296 1-km cells for each MM5 cell.

SHM and MM5 use the State Soil Geographic Database (STATSGO) dataset of soil types (Miller et al. 1994), where 1 of 12 soil types is assigned to each 1 km $\times$ 1 km cell covering the entire United States. Each of the 12 soil types is assigned values for hydraulic properties such as minimum soil suction, saturated conductivity, porosity, wilting point, and the beta parameter, which the models then use to calculate the vertical fluxes of soil moisture (section 2c). Land cover data were generated from the Global Land Cover Characteristic (GLCC) project operated by the EROS Data Center in 1997 (http://edcdaac.usgs.gov/glcc/glcc.html). Each grid cell is assigned 1 of 18 land cover classes that correspond to biophysical parameter estimates, according to a lookup table, such as leaf area density, roughness length, and albedo (BATS; Dickinson et al. 1986).

Initial fields of soil type (STATSGO) and land cover (GLCC) were used in both the SHM and MM5 simulations at 36-km grid spacing. Each was aggregated from 1 to 36 km by assigning the most frequent class or type occurring in each 36-km grid cell. These fields, along with the 36-km derived Fr and SWC fields (simulations 3 and 4), were uniformly interpolated by MM5 down to the grid spacing of the 12- and 4-km nests upon initialization. Although the land cover, soil type, and Fr data are available at 1-km grid spacing, we felt it crucial to keep consistency between SHM and MM5. This ensured that SWC estimated by SHM for a particular grid cell of, say, short grass, loam, and 26% Fr would be simulated in MM5 under the same conditions.

In SHM, the Clapp and Hornberger (CH; 1978) scheme is used, a portion of which is shown in the top part of Table 2, wherein the 12 STATSGO soil types and their associated soil parameter values are given. BATS and SHEELS, however, use the BATS table of hydraulic constants (bottom of Table 2), which differs from that of CH. BATS allows SWC to vary from the wilting point (residual SWC) of the soil, which ranges from 0.029 to 0.3575, to saturation, and CH allows SWC to vary from 0 to saturation. In addition, the values of saturation in BATS and CH are not equal. Therefore, the range of allowable SWC may differ significantly between models, and a rescaling of the soil moisture output from SHM was performed before it could be included in MM5 simulations:

$$\Theta_{\mathrm{MM5}} = \left(\frac{\Theta_{\mathrm{SHM}}}{\Theta_{s,\mathrm{CH}}}\right)(\Theta_{s,\mathrm{BATS}} - \Theta_{r,\mathrm{BATS}}) + \Theta_{r,\mathrm{BATS}}, \quad (7)$$

where $\Theta_{s,\mathrm{SHM}}$ is the soil water content from SHM, and the saturation (subscript s) and residual values (subscript r) are obtained from the BATS and CH soil parameterizations (Table 2). The SWC in the upper 10-cm layer of soil, if estimated as 0.235 from SHM, would be assigned a value of 0.261 for a silt loam soil upon initialization in MM5/SHEELS using this technique. The

TABLE 2. Upper (saturated) and lower (residual) limiting values of soil water content (Θ) and the beta parameters for the 12 STATSGO soil types, as specified by Clapp and Hornberger (1978; CH) and BATS (Dickinson et al. 1986).

Soil type	SWC_{sat} (Θ_s)	SWC_{min} (Θ_r)	b
CH			
Sand	0.395	0	3.5
Loamy sand	0.41	0	4.0
Sandy loam	0.435	0	4.5
Silt loam	0.485	0	5.0
Silt	0.485	0	5.5
Loam	0.451	0	6.0
Sandy clay loam	0.42	0	6.8
Silty clay loam	0.477	0	7.6
Clay loam	0.476	0	8.4
Sandy clay	0.426	0	9.2
Silty clay	0.492	0	10.0
Clay	0.482	0	10.8
BATS			
Sand	0.33	0.029	3.5
Loamy sand	0.36	0.0428	4.0
Sandy loam	0.39	0.0588	4.5
Silt loam	0.42	0.1117	5.0
Silt	0.45	0.1350	5.5
Loam	0.48	0.1592	6.0
Sandy clay loam	0.51	0.1926	6.8
Silty clay loam	0.54	0.2260	7.6
Clay loam	0.57	0.2592	8.4
Sandy clay	0.60	0.2922	9.2
Silty clay	0.63	0.3250	10.0
Clay	0.66	0.3575	10.8

ramifications of this rescaling between models will be discussed in section 6.

3. Simulation results: SWC

a. Soil moisture initialization

Although MM5/SHEELS resolves soil properties in 2-cm layers, SWC must be initialized in the model in the original BATS layers of an upper (0–10 cm), root zone, and deep soil layer down through 2 m. The 9-layer SWC data from SHM were aggregated into these 3 layers for use in simulation 4, and the upper 10-cm layer at initial time is shown in Fig. 2a for the 4-km nested domain. This aggregation of SHM data and loss of vertical resolution upon initialization will be discussed in section 6.

In comparison, the default 0–10-cm SWC initialized by MM5 in simulations 1, 2, and 3 is shown in Fig. 2b. The default SWC is purely a function of land cover type and date and is initialized from a lookup table in MM5/SHEELS. This default estimate gives a single value of SWC that is valid for the entire soil column at each grid cell, from the surface down through 2 m, and therefore lacks *any* vertical variability, the implications of which will be discussed in section 6. It is apparent that the spatial variability of soil moisture from SHM (Fig. 2a) is much higher than the default field generated for this date. The sharp gradients of SWC in both figures represent the soil type boundaries, corresponding to the gradients in hydraulic properties governed by soil type.

b. Near-surface soil drying

Soil moisture simulations show that some locations dry out quickly in the upper part of the five sublayers while others remain wet. Indeed, a large variability of drying rates can be seen throughout the ARM CART region in these simulations. Figure 3 shows two simulations of the upper five sublayers of SWC using derived SWC, labeled SHM, in one case and the default SWC, labeled FR, in another at Lamont, Oklahoma. The representative soil type here is listed as silt loam, and the vegetation fraction is 0.187. The lowest (driest) curves in each figure represent the uppermost (0–2 cm) soil layer. Through the first 24 h of the simulation, the default SWC shows much greater signs of decoupling, as the upper 2 cm dries out nearly 0.04 more than does the 8–10-cm layer. On the other hand, the derived SWC shows little variation in drying between layers through 24 h. Only late on the second afternoon does the simulation with the derived SWC begin to show more significant drying near the surface.

Figure 4 shows the upper five soil layers at Coldwater, Kansas, for the same two simulations. Coldwater is also located in a relatively bare soil region, with a vegetation cover of 0.257 and a soil type of loam. What is particularly noticeable at this location is the great amount of decoupling seen in using the derived values of SWC through the 36-h period. The derived SWC shows a decrease in the 0–2-cm layer of nearly 0.07 below that of the 8–10-cm layer and 0.03 below that of the 2–4-cm layer.

El Reno, Oklahoma, is another sparsely vegetated location with an Fr of 0.247 and silt loam soil. The soil moisture curves for the two simulations for El Reno are shown in Fig. 5. Here, the simulation with the derived SWC starts out much wetter again but shows no indication of decoupling at all during the 36-h simulation. The default SWC shows moderate decoupling, similar to that seen in Lamont, which has identical soil type and similar vegetation cover properties. The noticeable soil drying differences of the derived SWC simulations between Lamont and El Reno, particularly on day 2, are due to the initial SWC values. The derived SWC values at Lamont in the 0–10-cm layer are about 0.26; in El Reno the initial SWC is near 0.29.

c. Drying thresholds and soil type

At Lamont, the derived SWC values lead to decoupling on the second afternoon because, as suggested by CC97, the SWC reaches a threshold level for rapid drying in this soil type, whereas in El Reno the derived SWC remains too high for rapid drying to occur. Upon investigation we find that the degree of surface drying depends crucially on the initial SWC values. Figures

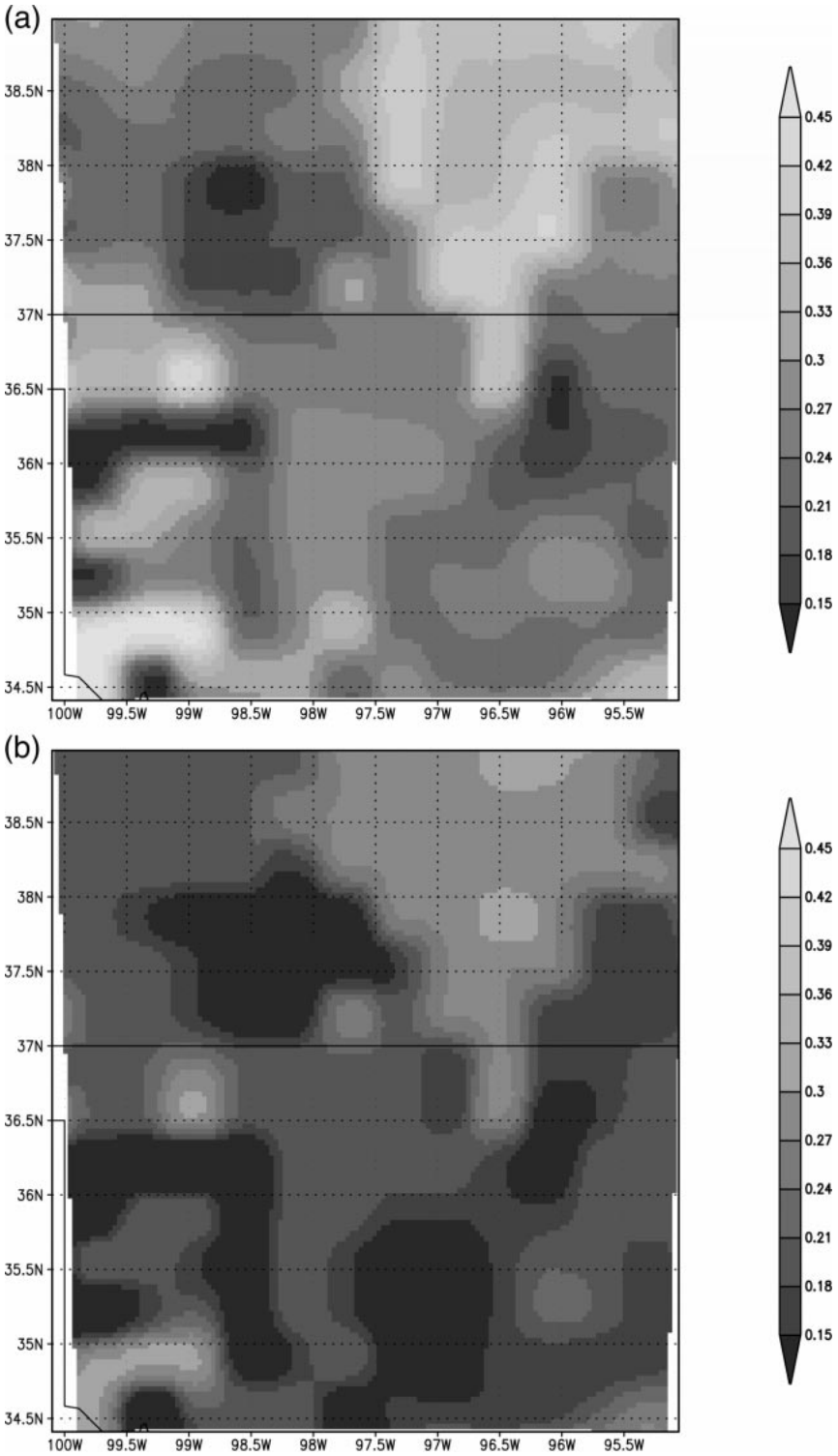

FIG. 2. Soil water content (Θ) of the 0–10-cm layer initialized in MM5/SHEELS at 1200 UTC 16 Jul 1996, derived from (a) SHM soil moisture profiles and (b) climatological estimates generated by default in MM5. This 4-km nested grid corresponds to that of the ARM CART project over central Oklahoma and Kansas.

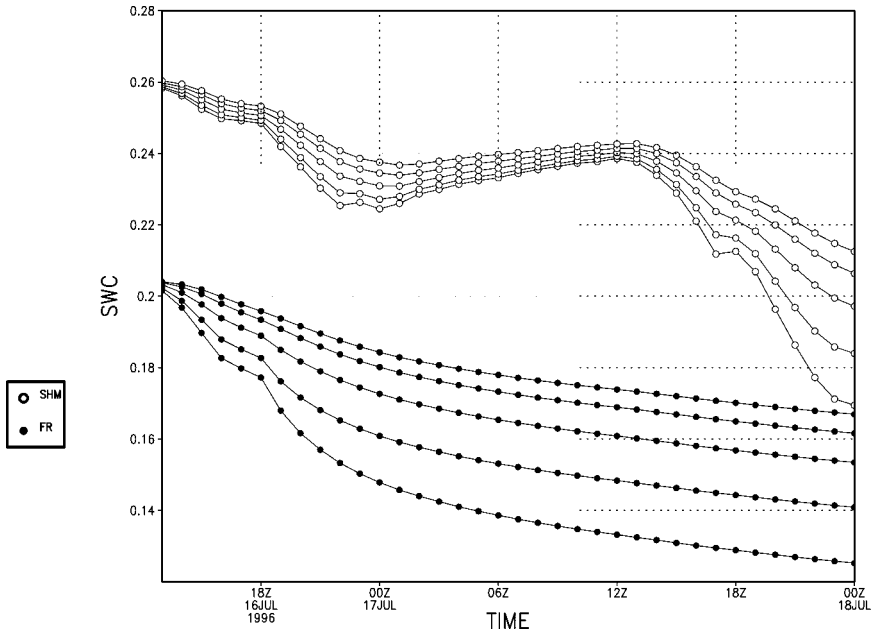

FIG. 3. Soil water content (Θ) of the upper five sublayers over the 36-h period for Lamont, OK. The open circles (SHM) represent the SHM-derived SWC simulation, the default SWC simulation is represented by closed circles (FR). The 0–2-cm layer (lowest curve) is the driest in each, and the 8–10-cm layer (highest curve) is the wet test.

3–5 show that MM5/SHEELS simulates rapid drying of near-surface soil layers only when the upper 10 cm of soil moisture resides in a certain threshold range that is highly dependent on the soil type.

Thresholds for different soil types can be determined by comparing drying rates and SWC values with soil type throughout the inner nest. When the rate of change of SWC for the 0–2-cm layer is significantly greater than that of the 8–10-cm layer, the value of SWC at which this divergence in drying rate first occurs is noted; this establishes an upper threshold range for a given soil type. A similar procedure determines the lower threshold limit. Table 3 gives the thresholds estimated from these simulations for the six soil types present in our

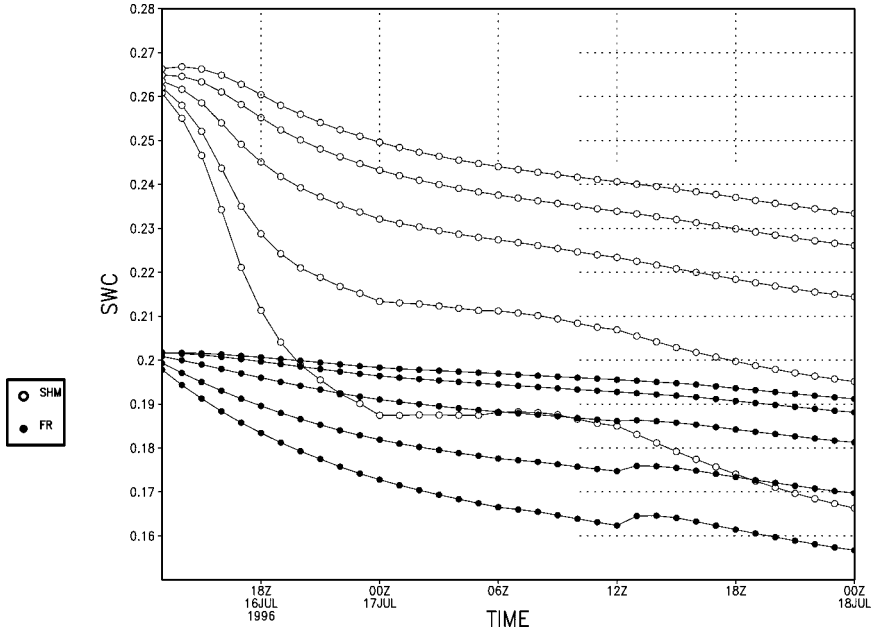

FIG. 4. Same as for Fig. 3 but for Coldwater, KS.

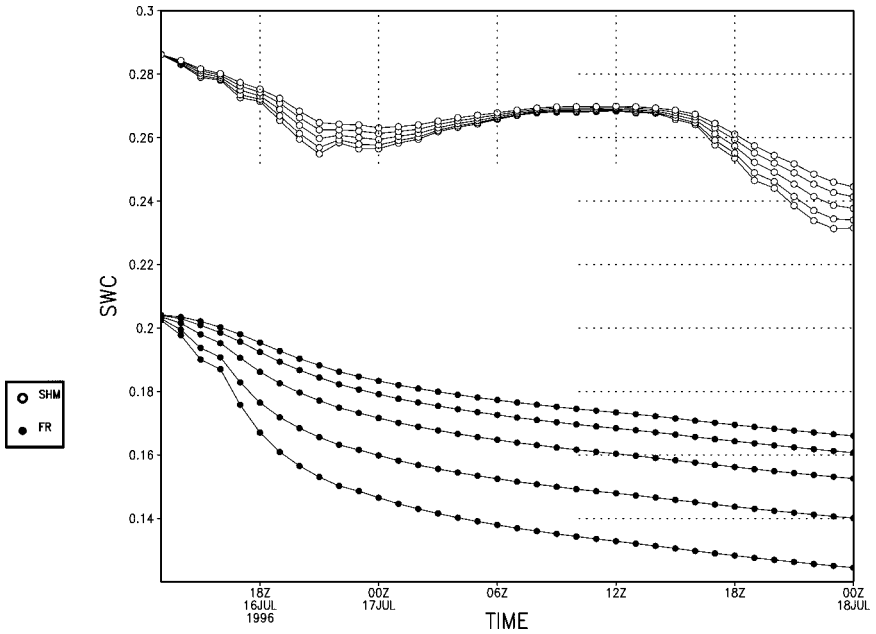

FIG. 5. Same as for Fig. 3 but for El Reno, OK.

domain. Classes such as silty clay loam and clay loam (soil types 8 and 9) tend to have higher threshold levels due to their higher saturation values. Consequently, simulations using the higher initial values of SWC (the simulations using the derived SWC) experience a more pronounced decoupling for soil types 8 and 9. The simulation with default soil moisture and derived Fr shows more rapid drying for soil types 1–4 because the typical default values of SWC lie in these lower threshold ranges.

Table 3 also lists the percent of saturation and field capacity for each soil type and corresponding threshold range. The upper limits of these thresholds range from 39.2% to 50.2% of saturation, and all but silt loam (49.1%) have ranges that include values of 50% of field capacity. This result is in agreement with an earlier study by CC97, who found similar thresholds for decoupling events using a different land surface scheme and hydraulic equations. Overall, rapid drying is likely if the initial SWC is between 13% and 50% of saturation, depending on the soil type and soil scheme used, and an SWC near 50% of field capacity almost always leads to rapid drying.

CC97 explain how the soil physics scheme [Eqs. (4–7)] governing the diffusion and evaporation of SWC can simulate decoupling. According to these equations, hydraulic conductivity varies with water content to the power of $3 + 2b$, and matric potential varies with water content to the $-b$ power, where b is empirically derived and assigned by soil type according to CH (1978). When a moist column of soil begins to evaporate, the hydraulic conductivity k decreases slowly while the matric potential gradient $\partial\psi/\partial z$ increases slowly. For very moist and dry values of θ, these changes in k and ψ tend to offset each other, keeping a constant upward flux of moisture and preventing rapid drying. However, as evaporation increases throughout the day, θ enters a middle range of SWC where the conductivity tends to decrease rapidly (according to the $3 + 2b$ power), and the matric potential gradient does not increase rapidly enough to compensate (according to the $-b$ power only). Therefore, the upward flux of moisture from the

TABLE 3. Threshold values (Θ_{dry}) and corresponding relative saturation and field capacity percentages of the upper 10 cm of SWC for each soil type that produce decoupled drying profiles of the upper soil layers.

Soil texture class	Θ_s (BATS—Table 2)	Initial SWC of drying events (Θ_{dry})	Relative SWC saturation % $(\Theta_{dry} - \Theta_r)/(\Theta_s - \Theta_r)$	% of field capacity $(\Theta_{dry} - \Theta_r)/0.75(\Theta_s - \Theta_r)$
1 (Sand)	0.33	0.10–0.17	23.6–46.8	31.5–62.4
3 (Sandy loam)	0.39	0.170–0.225	33.6–50.2	44.8–66.9
4 (Silt loam)	0.42	0.175–0.225	20.5–36.8	27.3–49.1
6 (Loam)	0.48	0.235–0.285	23.6–39.2	31.5–52.3
8 (Silty clay loam)	0.54	0.27–0.35	14.1–39.5	18.8–52.7
9 (Clay loam)	0.57	0.30–0.40	13.1–45.3	17.5–60.4

lower soil layers is retarded according to Eq. (3). This process continues as the upper soil layer continues to evaporate at a high rate but is not replenished from below, and it therefore dries out considerably more than the lower layers. The lower threshold limit occurs when evaporative demand decreases because of the dryness of the soil (as determined by the evaporative weighting scheme).

Thus, decoupling is not seen in soils that are already dry or near saturation. That the exact threshold ranges are strictly a function of the soil type (*b*) suggests that rapid soil drying is sensitive to the choice of parameterization. Because the surface drying profoundly affects the surface temperature and moisture, differing threshold ranges may produce significant differences in sensible and latent heat fluxes. CC97 show that a change in the *b* parameter in the soil water flux equation (CH) of only one standard deviation within a single soil type results in differences in the drying rates of the soil layers that are almost as significant as those between soil types. Therefore, it is not so much the actual threshold values that are of importance in these results. What these results do show is the close dependence of initial SWC and drying rates simulated in land surface schemes on the parameterization of soil type and on the choice of soil parameters.

4. Simulation results: Fr

a. Overall fractional vegetation cover fields

The NDVI-derived Fr field over the ARM CART (4 km) domain for the period 5–19 July 1996, shown in Fig. 6a, exhibits great spatial detail in capturing the sharp east–west gradient of Fr. Figure 6b shows the default Fr over the same region on 16 July 1996. Default Fr is initialized in MM5/SHEELS from a lookup table and is a function of subsurface soil temperature, land cover type, and a seasonal range of vegetation cover, as in the original BATS (Dickinson et al. 1986). The homogeneous nature of Fr, which is mostly above 0.8 because of the uniformly high temperatures of July, fails to capture the actual spatial variation in vegetation that exists over the western half of the central Great Plains region.

b. Impacts of Fr on MM5/SHEELS simulations: Temporal evolution of soil moisture

Figures 7a,b show the 0–2-cm soil water content for simulations 3 and 2, respectively, along the 36.17°N latitude stripe over the 36-h period. The simulations are identical except for the Fr field initialized in each (derived, Fig. 7a, or default, Fig. 7b). In both figures, sharp horizontal gradients in SWC result from the imposition of soil type gradients across the latitude stripe. With default values of Fr, the SWC remains high, and rapid drying is absent. With derived Fr, a wide area of rapid drying is evident in the middle of the segment, and a check of the SWC profiles in the region confirms that decoupling does occur here. This central area of drying corresponds to a soil type of silt loam and to an initial SWC (identical in each run) within the corresponding threshold range for decoupling. The derived Fr gives less than 0.3 (30%) vegetation cover (Fig. 8) for this central region and so results in significant evaporation from a largely bare soil surface. The default vegetation cover for this area remains above 0.8 (80%); the upper soil layers, therefore, do not dry out as quickly, despite the initial SWC being within the drying threshold range.

On the eastern edge of the domain, the soil type is also silt loam, and the initial SWC is within the threshold range for rapid drying, as in the central region. However, drying is much less evident and much slower in this area with derived Fr than in the central portion, with only a slight decoupling (not shown) of the soil. This result is due to the higher values of Fr (above 0.60) along the eastern edge of the cross section, which limits the amount of bare-soil evaporation. The remainder of the cross section experiences little drying, because the initial SWC values of the simulations are not within the threshold ranges for decoupling.

c. Consequences of soil drying due to vegetation cover variations

Soil drying manifests itself in the surface fluxes and the surface temperatures. Figure 9 shows the sensible heat fluxes across the 36.17° latitude stripe at 1900 UTC on 17 July 1996, approximately midafternoon on the second day of the simulation when considerable drying has already occurred. The simulation with derived Fr shows generally larger sensible heat fluxes than that with the default Fr, the greatest differences (greater than a factor of 2) occurring in the central region where decoupling is most pronounced. Both simulations show nearly equal fluxes along the eastern border, where derived and default Fr are both large. The latent heat fluxes (not shown) exhibit the opposite behavior, as expected.

Surface skin temperatures, simulated for the 4-km domain at late afternoon on the second day of the simulations, are shown in Figs. 10a (derived Fr) and 10b (default Fr). Derived Fr (Fig. 10a) produces markedly higher surface temperatures than the simulation with climatological Fr (Fig. 10b), with the exception of the eastern and southeastern edges. The temperature pattern inversely corresponds with the distribution of Fr (Figs. 6a,b), and therefore reflects the percentage of bare soil present in each grid cell. The variability within the western half of the domain in each simulation reflects the happenstance distribution of the drying threshold, which is a function of the soil type.

5. Validation of MM5/SHEELS simulations

Air temperature measurements from the ARM CART domain were examined on a point-by-point basis and compared with simulated values for those locations. Fig-

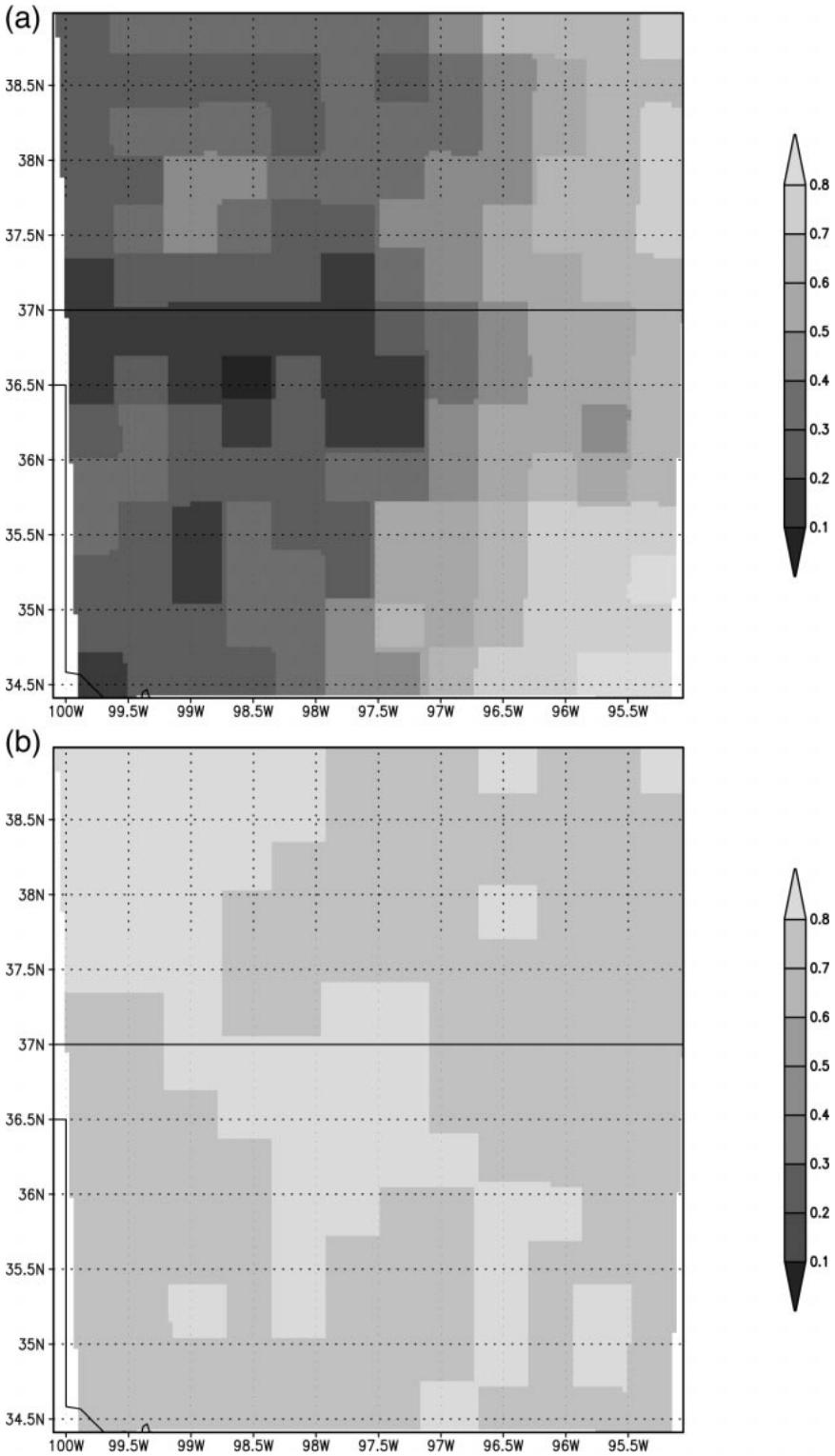

FIG. 6. Fractional vegetation cover for the 4-km domain over the 36-h period derived from (a) NDVI composites and (b) default estimates generated by MM5. These plots are identical to Figs. 1a and 1b except that the data have been interpolated down to the 4-km nested domain.

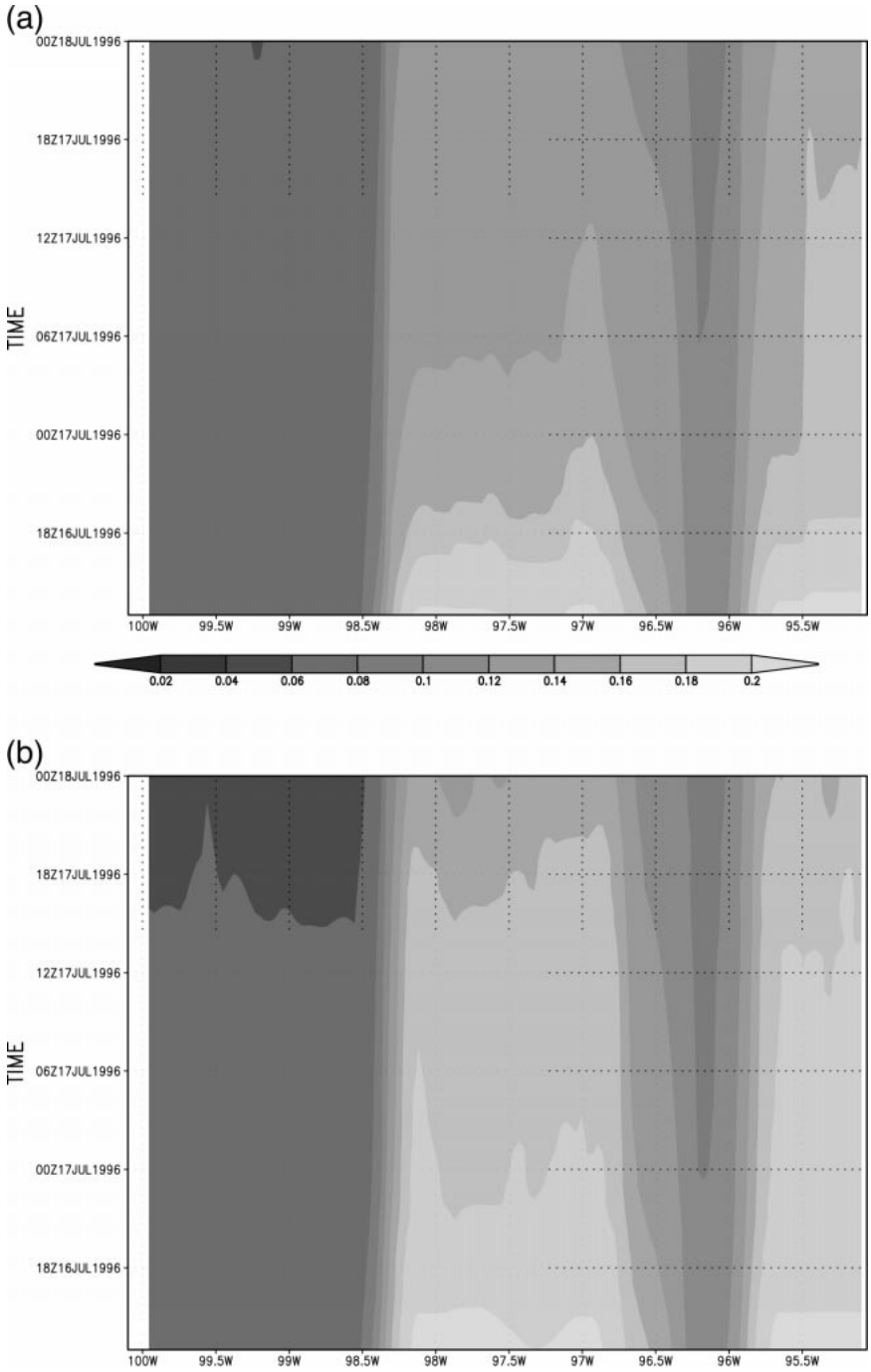

FIG. 7. SWC along the 36.17°N latitude stripe of the 4-km domain, showing 0–2-cm SWC as a function of time (increasing upward) and distance for the (a) NDVI-derived Fr and (b) default Fr simulations during the 36-h period. Note the rapid drying evident in the central portion of the cross section for the derived Fr simulation.

ure 11 shows the temperature curves of the four simulations and the corresponding observations over the 36-h period for Lamont. Simulation 3 clearly yields the closest agreement, particularly in the maximum values. The calculated rmses of the four simulations are as follows: 1 = 2.562, 2 = 2.320, 3 = 1.729, and 4 = 3.245. All four simulations yield minimum temperatures above the observed, with those using derived SWC being closest, but not within 2°C of the observed minimums.

Soil moisture profiles from simulations with default versus derived SWC are presented for this station in Fig. 3. The former shows decoupling at this location

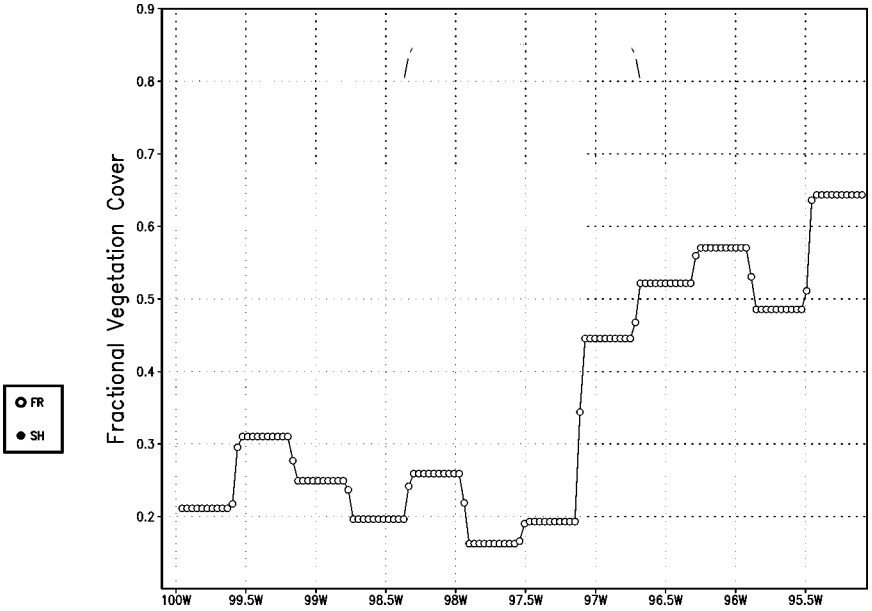

FIG. 8. Fractional vegetation cover along the 36.17°N latitude stripe. The open circles (FR) represent derived (NDVI based) vegetation cover; the closed circles (SH) represent default vegetation cover. Here, Fr is constant over the 36-h period because the 2-week composites of NDVI data and slow climatological variability of default estimates yield consistent Fr throughout.

throughout the 36-h simulation, and the latter only begins to dry out at the very end of the period. This decoupling of the default SWC results in a large increase in sensible heat flux on both afternoons and, therefore, higher maximum temperatures. The derived SWC, much wetter down through the root zone, yields large evaporation and transpiration rates on day 1. When the upper soil starts to dry out late on the second day, however, the latent heat flux begins to diminish with time, and the sensible heat flux increases (not shown). It is likely that this drying would have led to decoupling on the third day, thereby reducing the forecast errors for the simulation with derived SWC.

Measurements of SWC at 2.5 cm (0–5-cm SWC av-

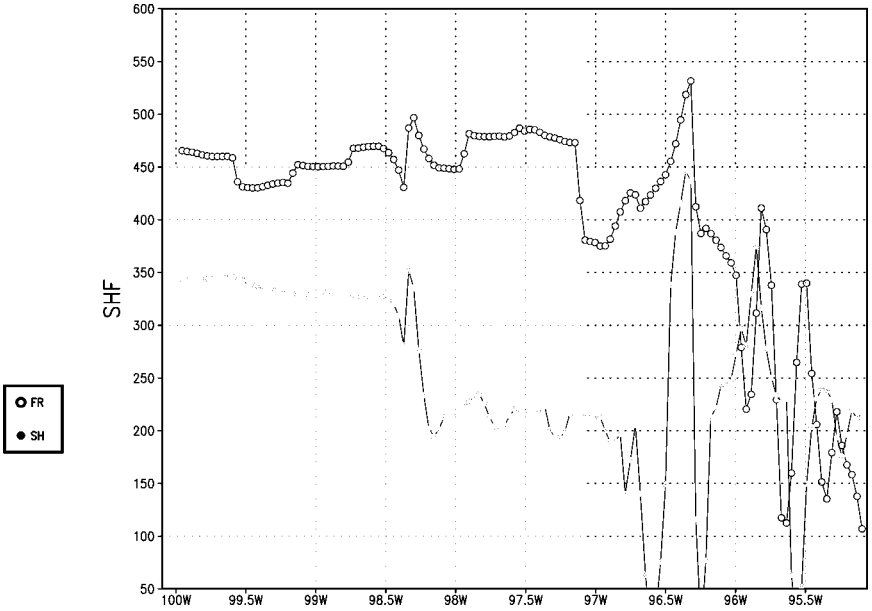

FIG. 9. Sensible heat flux (W m^{-2}) across the 36.17°N latitude stripe at 1900 UTC 18 Jul 1996. Open circles (FR) represent the derived (NDVI-based) vegetation cover simulation; the closed circles (SH) represent the default vegetation cover simulation.

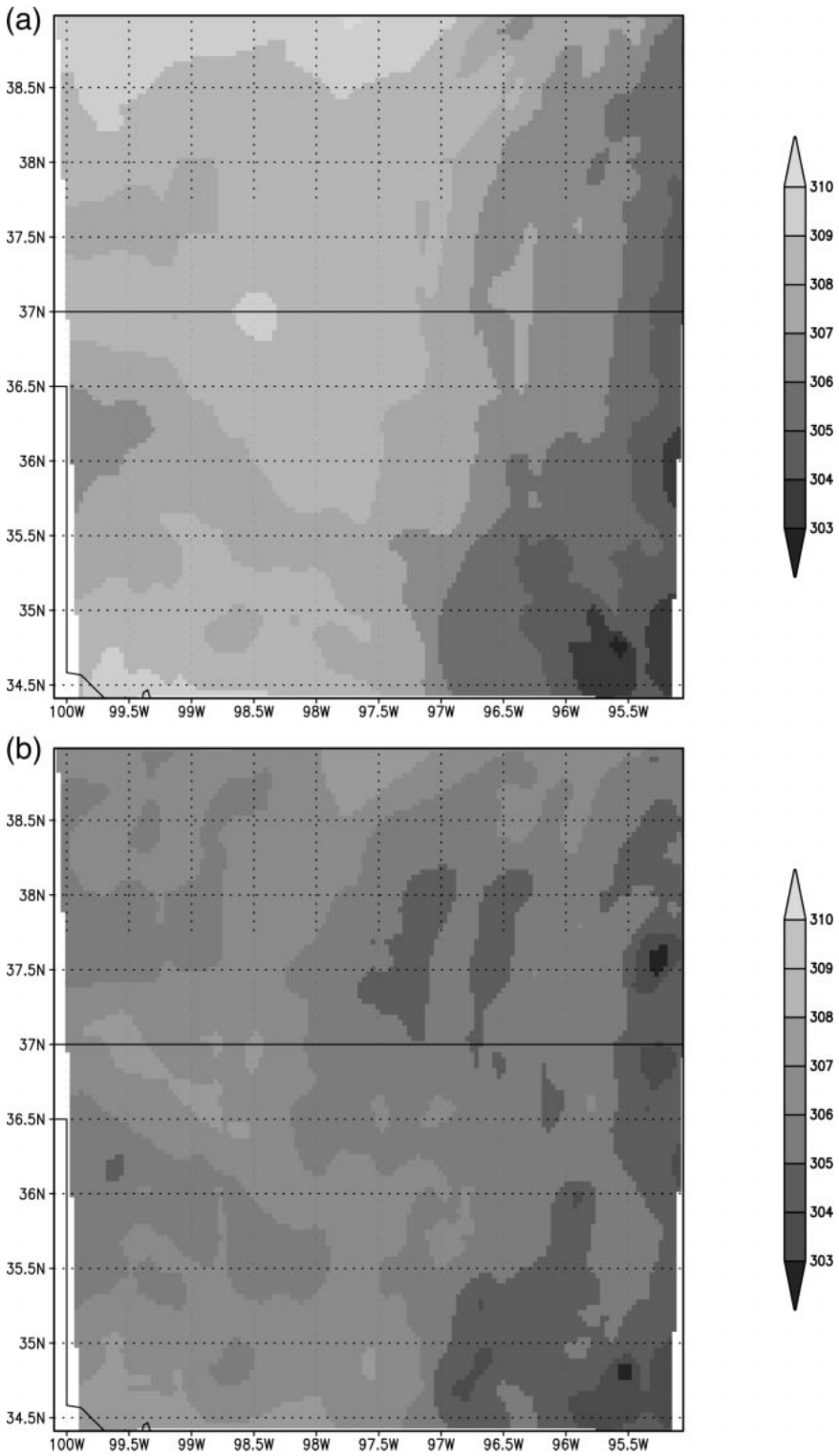

FIG. 10. Surface skin temperature (K) over the 4-km domain at 2200 UTC 17 Jul 1996 for the (a) NDVI-derived Fr and (b) default Fr simulations.

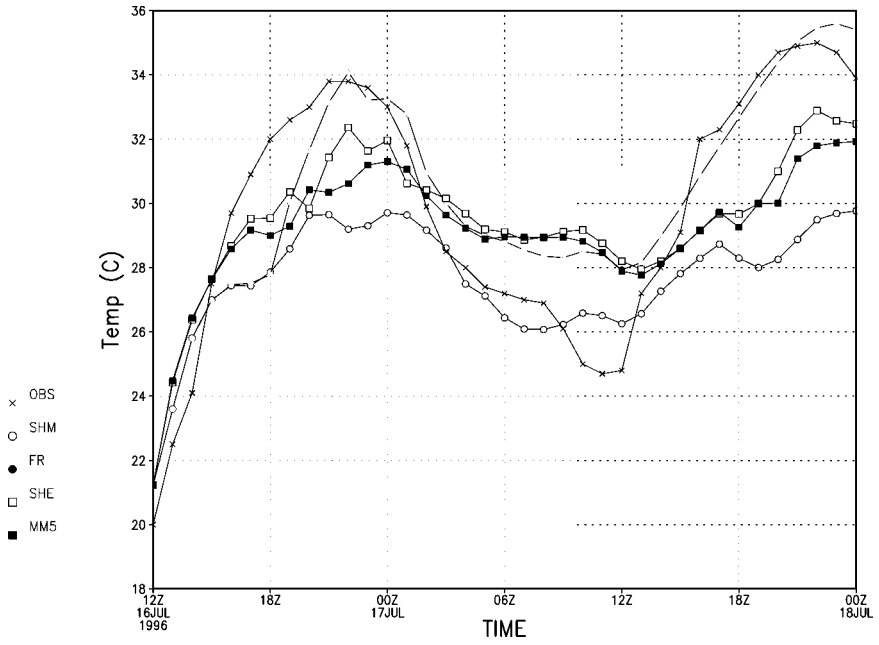

FIG. 11. Simulated (simulations 1–4) and measured (OBS) air temperature for Lamont, OK, over the 36-h period. Refer to Table 1 for the input parameters used in simulations 1 (here labeled ''MM5''), 2 (''SHE''), 3 (''FR''), and 4 (''SHM'').

erages measured in plastic bags) from this site show a slow decrease from 0.29- to 0.25Θ, followed by a more rapid drying trend beginning in the 0.20–0.23 range by the second afternoon. This observed drying may reflect a threshold for this soil type, consistent with the estimate of 0.175–0.225 derived from the simulations. According to these measurements, the simulation with default SWC provides a better temperature simulation because its values happen to coincide with the decoupling threshold.

The 12 other ARM CART facilities display almost identical patterns to that of Lamont. The simulation with default SWC and derived Fr yields good results for the afternoon temperatures; those with the derived SWC from the SHM were the least accurate, with errors as large as 6°C. The fact that these two runs differ only in the initial soil moisture and yield such dissimilar results underscores the importance of the SWC parameter in land surface models. Even when simulations with the derived SWC exhibit decoupling, which occurs only on day 2 in most cases, temperatures are unable to reach those higher values reported in the observations because of the high evaporation and low temperatures on day 1. Simulations 1 and 2, although they may contain the more accurate (default) surface soil moisture, are greatly affected by the high values of default Fr (>0.8) and are consistently 1°–2°C cooler than those with the derived Fr.

Overall, there was little consistent evidence of agreement between any one simulation and the measured soil moisture, dewpoint temperatures, or fluxes. This result may be due to the point versus area mismatch in scales, particularly with surface fluxes, which tend to have great fluctuations at a point but smooth out over larger areas. In view of the possible errors in the SWC, dewpoint, and temperature measurements at these points, these validations are, at best, tentative, and the only consistency was seen in the air temperature comparisons.

6. Discussion of results and complicating issues

a. Generation of soil moisture fields

The SHM was responding to a recent precipitation event, which generated SWC values much higher than the default SWC values from MM5/SHEELS. Because BATS considers a higher range of SWC than the CH values (Table 2), the soil moisture from SHM was scaled up even more [Eq. (1)], thus amplifying the differences between the default and derived fields. Thus, the inaccuracy of the SHM values, in terms of resulting temperature validations, may be an artifact of the data reduction process.

In addition to the ambiguity created by scaling, a further source of uncertainty in initializing the 9-layer SHM output was that the latter had to be aggregated into three discrete layers for input into MM5/SHEELS, the topmost being 0–10 cm. For this particular study, not much was lost in this aggregation, because the initialization time is postprecipitation when fairly uniform soil profiles were present (0.234, 0.235, and 0.236 at Lamont for the top three SHM layers composing the 0–10-cm layer). Had we been investigating an already dry soil surface, such as the one simulated by SHM for 18 July, this issue would have created a much larger

problem, and SHEELS is being reformulated to account for flexible soil layering at initialization as a result.

There is also the problem created by the default SWC being vertically constant from the surface through 2 m as generated by MM5 for the default SWC simulations. A look at the FR simulations in Figs. 3–5 shows a definite lack of the diurnal variability seen in the SHM simulation. Because of the constant initial SWC profile, there is not enough of a gradient of SWC from the upper layers to the root zone to generate a recharge overnight (towards the surface) of moisture. The initial profile of derived SWC is considerably more moist in the root zone and acts to drive this recharge according to the flow equations presented earlier. Although the default profile simulates better temperatures in the end, this result is only due to the initially drier near-surface soil layer; longer timescales might have yielded different results.

Regardless of which method of determining SWC is more accurate, modeled or default, our results demonstrate the importance of initial conditions on the future drying of the soil. Future studies linking hydrologically derived SWC with mesoscale models should consider using identical hydraulic schemes to eliminate the need for and possible problems of rescaling SWC data and should consider the use of consistent soil layers between hydrologic and mesoscale soil modeling.

SHM-generated profiles do have three distinct advantages over derived SWC profiles with regard to the issues above: 1) Modeled SWC is not climatological and is driven by actual meteorological forcings, 2) There is vertical variation in SWC profiles from SHM, which can contribute immediately to vertical moisture fluxes in a coupled model, and c) SHM can give an indication of when and where decoupling may be likely by looking at the SWC with soil types.

b. Generation of fractional vegetation cover data

Clearly, Fr estimates generated here are an improvement in both time and space over default estimates. As evidenced in the results, an improvement in simulating afternoon temperatures occurs when a more detailed vegetation field is initialized, although the initial condition of near-surface soil moisture is often more important than the vegetation amount (unless there is nearly complete vegetation cover, in which case transpiration and root-zone SWC will dominate).

c. Simulation of decoupling

Results indicate that improved soil moisture data do not necessarily yield more accurate simulations of land surface processes, because of uncertainties in soil type and vegetation parameterizations. Higher SWC, such as that generated by the SHM, may lie above the decoupling threshold range, which is governed by the hydraulic constants in SHEELS. In that instance, the soil may dry out too slowly for the surface temperatures to respond correctly.

Decoupling has not been widely noted in mesoscale simulations, suggesting not only that it occurs for a limited range of conditions, but that existing models have had insufficient substrate resolution to describe it. Because decoupling is so critically dependent on resolution, initial SWC, soil type, Fr, and insolation, it remains a challenge to predict where and when it will occur. This challenge is illustrated by Fig. 5. When the SWC is above the threshold range, drying is relatively slow for the SHM-derived SWC simulation. In this case the depth of the shallow surface soil layer is virtually irrelevant, and the precise value of SWC is of little importance except insofar as it was above the threshold range. Similarly, when Fr is large (or the sky is overcast) the threshold range or substrate drying depth is irrelevant. For that reason, the increased spatial detail in the derived Fr may yet prove to be more useful than the SWC values.

These results underscore the importance of soil type, which is a controlling factor in determining the hydraulic conductivity and, therefore, the threshold drying range. The problem in predicting decoupling, however, may remain indeterminate, because the composition of soils is actually a mixture of different types. SWC measurements taken at five locations within 20 m of each other at an individual ARM CART station can exhibit variations of SWC on the order of 50% of each other due to differential drying and soil types across the site. It is tempting to believe that higher spatial resolution in mesoscale models may better resolve spatially heterogeneous soil layers, but the variable nature of soils and soil water content (on the order of 1 m) may make this goal impossible. Moreover, it is not obvious how one averages soil properties in such an inhomogeneous mixture, and a similar problem also presents itself in averaging Fr. At the heart of the averaging problem is the hugely nonlinear relationship between soil hydraulic conductivity and soil water content.

7. Conclusions

Although we have not demonstrated that a derived SWC is necessarily superior to a default value, the paper does underscore the importance of rapid surface drying (decoupling) in prescribing the surface energy budget. Introduction of a derived Fr, however, does appear to be useful in predicting rapid soil drying. Rapid drying of near-surface soil was simulated by MM5/SHEELS in many locations during this case study, particularly where vegetation cover was less than 0.6. Given strong insolation, and a vegetation cover less than 0.6, decoupling occurs where the initial soil water content in the top 10 cm lies within a threshold range (typically between about one-quarter and one-half of soil saturation) determined by soil type. Based on simulations for the ARM CART SGP site in central Kansas and Oklahoma,

these SWC threshold ranges were determined for various soil types.

Rapid drying was accompanied by an increase in sensible heat flux, surface skin temperatures, and daily maximum air temperatures. Although decoupling was evidenced in all four simulations at one location or another, the SHM-derived soil moisture remained mostly above the threshold range, in contrast to the lower default SWC from climatological values. The most accurate temperature forecasts were simulated using the derived Fr and default soil moisture fields. Largest errors in maximum temperature were found for the derived Fr and the derived SWC, which contributed to more evapotranspiration and less surface heating than for simulations with the default values.

The key points in this paper about the simulation of rapid surface drying in the ARM CART SGP site covering central Kansas and Oklahoma are as follows.

1) Fractional vegetation cover derived from biweekly, remotely sensed NDVI data provides some improvement over default estimates.
2) Soil moisture simulated from a hydrological model with finely resolved vertical resolution shows signs of decoupling of the soil layers under appropriate atmospheric conditions. However, these values of soil moisture are particularly sensitive to the soil parameterization and soil type.
3) Higher–vertical resolution soil models, such as that used in SHEELS, have the ability to simulate rapid drying of the upper soil layers model at each point.
4) Rapid soil drying (decoupling) occurs within the 0–2-cm layer when the average SWC over the top 10 cm falls into certain threshold ranges that are dependent on soil type.
5) The effect of near-surface SWC and soil type is much larger than that of Fr, with the exception of regions where Fr exceeds 80% and therefore vegetation and root-zone soil moisture are dominant. More accurate specification of vegetation fraction improved the forecasts overall, but the derived SWC produced large errors in simulated temperatures, possibly because of an incorrect interpolation from SHM to SHEELS.
6) Future modifications to SHEELS will ensure that more realistic SWC will be included. The accuracy of such models, however, may be limited by the inherent local-scale variability of soil type and SWC and the highly nonlinear behavior of soil hydraulic conductivity as a function of SWC.

Points 1–4 suggest that much improvement in land surface parameterization can be accomplished through remote estimation of large-scale biophysical properties. Above all, it is necessary to include a high-resolution soil model to capture decoupling. Increased data resolution and availability will make it even easier in the future to simulate soil drying at smaller scales, as new relationships between remotely sensed indices and biophysical variables can be developed.

Points 5 and 6 introduce a note of caution, that is, that the increased complexity of land surface schemes and measurements does not always result in improved predictions. Soil moisture and soil-type data are so crucial for predicting decoupling and so spatially variable that the problem of predicting decoupling may be indeterminate. An important goal, nevertheless, is to improve the land surface schemes along with obtaining better estimates of soil and vegetation data.

Acknowledgments. Technical assistance throughout this study was provided in the meteorology department by David Ripley, Eugene Clothiaux, Glenn Hunter, Richard White, Bill Peterson, Robert Hart, and George Bryan. SHM simulations were performed by Mercedes Lakhtakia and Richard White of the Earth System Science Center at PSU. Many thanks go out to Bill Lapenta, Bill Crosson, and Scott Dembek from NASA/MSFC in Huntsville, Alabama, for their development and modification of SHEELS. All research was funded by United States Air Force Grant F49620-95-1-0255.

REFERENCES

Anthes, R. A., and T. T. Warner, 1978: Development of hydrodynamic models suitable for air pollution and other mesometeorological studies. *Mon. Wea. Rev.,* **106,** 1045–1078.

Brutsaert, W., and D. Chen, 1995: Desorption and the two stages of drying of natural tallgrass prairie. *Water Resour. Res.,* **31,** 1305–1313.

Capehart, W. J., 1996: Issues regarding the remote sensing and modeling of soil moisture for meteorological applications. Ph.D. thesis, The Pennsylvania State University, 239 pp. [Available from Institute of Atmospheric Sciences, South Dakota School of Mines and Technology, Rapid City, SD 57701; william.capehart@sdsmt.edu.]

——, and T. N. Carlson, 1994: Estimating near-surface moisture availability using a meteorologically driven soil-water profile model. *J. Hydrol.,* **160,** 1–20.

——, and ——, 1997: Decoupling of surface and near-surface soil water content: A remote sensing perspective. *Water Resour. Res.,* **33,** 1383–1395.

Carlson, T. N., and D. A. J. Ripley, 1997: On the relation between NDVI, fractional vegetation cover, and leaf area index. *Remote Sens. Environ.,* **62,** 241–252.

——, ——, and T. J. Schmugge, 2000: Rapid soil drying and its implications for remote sensing of soil moisture and the surface energy fluxes. *Thermal Remote Sensing in Land Surface Processes,* Ann Arbor Press, in press.

Choudhury, B. J., A. U. Ahmed, S. B. Idso, R. J. Reginato, and C. S. T. Daughtry, 1994: Relations between evaporation coefficients and vegetation indices studied by model simulations. *Remote Sens. Environ.,* **50,** 1–17.

Clapp, R. B., and G. M. Hornberger, 1978: Empirical equations for some soil hydraulic properties. *Water Resour. Res.,* **14,** 601–604.

Crawford, T., D. J. Stensrud, T. N. Carlson, and W. J. Capehart, 2000: Using a soil hydrology model to obtain regionally averaged soil moisture values. *J. Hydrometeor.,* **1,** 353–363.

Dickinson, R. E., A. Henderson-Sellers, P. J. Kennedy, and M. F. Wilson, 1986: Biosphere–Atmosphere Transfer Scheme (BATS) for the NCAR Community Climate Model. NCAR Tech. Note

NCAR/TN-275 + STR, 69 pp. [Available from UCAR Communications, P.O. Box 3000, Boulder, CO 80307-3000.]

Gillies, R. R., and T. N. Carlson, 1995: Thermal remote sensing of surface soil water content with partial vegetation cover for incorporation into climate models. *J. Appl. Meteor.*, **34,** 745–756.

——, ——, J. Cui, W. P. Kustas, and K. S. Humes, 1997: A verification of the ''triangle'' method for obtaining surface soil water content and energy fluxes from remote measurements of the normalized difference vegetation index (NDVI) and surface radiant temperature. *Int. J. Remote Sens.*, **18,** 3145–3166.

Idso, S. B., R. J. Reginato, R. D. Jackson, B. A. Kimball, and F. S. Nakayama, 1974: The three stages of drying of a field soil. *Soil Sci. Soc. Amer. Proc.*, **23,** 183–187.

Jackson, R. D., 1973: Diurnal changes in soil water content during drying. *Field Soil Water Regime: Proceedings of Symposium,* R. R. Bruce et al., Eds., American Society of Agronomy, 37–55.

Kustas, W. P., and J. M. Norman, 1999: Evaluation of soil and vegetation heat flux predictions using a simple two-source model with radiometric temperatures for a partial canopy cover. *Agric. For. Meteor.*, **94,** 13–29.

Lapenta W., M. Lakhtakia, W. Crosson, and S. Dembek, 1998: Penn State/NCAR Mesoscale Model (MM5). *Global Water Cycle: Extension Across the Earth Sciences (NASA EOS Progress Report).* The Pennsylvania State University, 12–19. [Available online at http://dbwww.essc.psu.edu/reports/NASA_Report_1997.pdf.]

McCumber, M. C., and R. A. Pielke, 1981: Simulation of the effects of surface fluxes of heat and moisture in a mesoscale numerical model. *J. Geophys. Res.*, **86,** 9929–9938.

Miller, D. A., G. W. Peterson, and M. N. Lakhtakia, 1994: Using the State Soil Geographic Database (STATSGO) for regional atmospheric modeling. *Agronomy Abstracts, Annual Meeting of the Soil Science Society of America,* Seattle, WA, SSSA, 249 pp.

Milly, P. C. D., 1982: Moisture and heat transport in hysteretic, inhomogeneous porous media: A matric head-based formulation and a numerical model. *Water Resour. Res.*, **18,** 489–498.

——, 1984: A simulation analysis of thermal effects on evaporation from soil. *Water Resour. Res.*, **20,** 1087–1098.

Saravanapavan, T., and G. D. Salvucci, 2000: Analysis of rate-limiting processes in soil evaporation with implications for soil resistance models. *Adv. Water Res.*, **23,** 493–502.

Smith, C. B., M. N. Lakhtakia, W. J. Capehart, and T. N. Carlson, 1994: Initialization of soil-water content in regional-scale atmospheric prediction models. *Bull. Amer. Meteor. Soc.*, **75,** 585–593.

Sun, W. Y., and M. G. Bosilovich, 1996: Planetary boundary layer and surface layer sensitivity to land surface parameters. *Bound.-Layer Meteor.*, **77,** 353–378.